Heliyon 9 (2023) e14281

Contents lists available at ScienceDirect

Heliyon

journal homepage: www.cell.com/heliyon

Research article

Development and *in-vitro* evaluation of chitosan and glyceryl monostearate based matrix lipid polymer hybrid nanoparticles (LPHNPs) for oral delivery of itraconazole

Rimsha Yousaf [a], Muhammad Imran Khan [a,**], Muhammad Furqan Akhtar [a,*], Asadullah Madni [b], Muhammad Farhan Sohail [a], Ammara Saleem [c], Kanwal Irshad [d], Ali Sharif [e], Maria Rana [a]

[a] *Riphah Institute of Pharmaceutical Sciences, Riphah International University, Lahore Campus, 54000, Lahore, Pakistan*
[b] *Department of Pharmaceutics, Faculty of Pharmacy, The Islamia University of Bahawalpur, Bahawalpur, 63100, Pakistan*
[c] *Department of Pharmacology, Faculty of Pharmaceutical Sciences, Government College University Faisalabad, Pakistan*
[d] *Department of Pharmaceutical Chemistry, Faculty of Pharmaceutical Sciences, Government College University Faisalabad, Pakistan*
[e] *Institute of Pharmacy, Faculty of Pharmaceutical and Allied Health Sciences, Lahore College for Women University, Lahore, Pakistan*

ARTICLE INFO

Keywords:
Itraconazole
Chitosan
Glyceryl monostearte
Poloxamer 188
Lipid-polymer hybrid nanoparticles
Dissolution enhancement

ABSTRACT

Itraconazole (ICZ) is a broad spectrum antifungal drug, but used as second or third line therapy due to its low and erratic oral bioavailability. This work was carried out to prepare and characterize matrix type lipid-polymer hybrid nanoparticles (LPHNPs) for dissolution enhancement of ICZ. LPHNPs were prepared using solvent diffusion/emulsification technique. Matrix LPHNPs were composed of chitosan (polymer), glyceryl monostearate (lipid) and poloxamer 188 (stabilizer). LPHNPs loaded with ICZ (LPHNPs-1, LPHNPs-2, LPHNPs-3 and LPHNPs-4) were developed using varying concentration of chitosan whereas LPHNPs (LPHNPs-5, LPHNPs-6, LPHNPs-7 and LPHNPs-8) were prepared using varying concentrations of poloxamer 188. LPHNPs loaded with ICZ were further evaluated for entrapment efficiency, particle size, polydispersity index (PDI), zeta potential and dissolution profiles at biorelevant pH conditions. The particle size (LPHNPs-1 to LPHNPs-4) was found to be in range of 421–588 nm with PDI values 0.34–0.41. The particles size of LPHNPs-5 to LPHNPs-8 was found to be in range of 489–725 nm with PDI 0.34–0.74. The entrapment efficiency of LPHNPs-1 to LPHNPs-4 was found to be in range of 85.21%–91.34%. The entrapment efficiency of LPHNPs-5 to LPHNPs-8 was found to be in range 78.32%–90.44%. . The scanning electron microscopy of optimized formulations LPHNPs-1 and LPHNPs-5 indicated formation of oval shaped nanoparticles. DSC thermogram of ICZ loaded LPHNPs also depicted the conversion of crystalline form of ICZ into amorphous form demonstrating the internalization and dissolution enhancement of drug in the hybrid matrix. The cumulative drug dissolved at acidic pH 1.2 was found to be 23.3% and 19.8% for LPHNPs-1 and LPHNPs-5 respectively. Similarly at basic pH values 7.4, cumulative amount of drug dissolved was 90.2% and 83.4% for LPHNPs-1 and LPHNPs-5 respectively. Drug dissolution kinetics exhibited fickian diffusion best described by Korse-meyer Peppas model. The results suggested that chitosan and glyceryl monostearate based

Abbreviations: Itraconazole, ICZ; Lipid-polymer hybrid nanoparticles, LPHNPs; Biopharmaceutical classification system, BCS; Glyceryl monostearate, GMS; attenuated total reflectance Fourier transform infrared spectroscopy, ATR-FTIR.

* Corresponding author.
** Corresponding author.
E-mail addresses: Imran.khan@riphah.edu.pk (M.I. Khan), mfurqan.akhtar@riphah.edu.pk (M.F. Akhtar).

https://doi.org/10.1016/j.heliyon.2023.e14281
Received 30 November 2022; Received in revised form 23 February 2023; Accepted 1 March 2023
Available online 9 March 2023

matrix LPHNPs could be used as promising approach for dissolution enhancement of ICZ which could further increase its bioavailability.

1. Introduction

Itraconazole (ICZ) belongs to Biopharmaceutical classification system II drugs having low water-solubility leading to erratic oral bioavailability. It has broad antifungal spectrum against a variety of fungus strains causing the opportunistic infection [1]. ICZ is a weak basic drug (pKa = 3.7) which is virtually ionized at low pH, showing extremely low water solubility values, about 1 ng/mL at neutral pH and about 4–6 μg/mL at acidic pH 1 [2]. Because of its poor aqueous solubility, its absolute oral bioavailability is only 55% [3]. The low oral bioavailability hampers its widespread use in clinical practices. Over the last decade, extensive research has been conducted with drug delivery approaches for poorly water-soluble and lipophilic drugs, including solid dispersions, emulsion based systems and nanoparticulate based dosage forms [4]. Recently, nanotechnology has emerged as the most promising tool in the fabrication of novel drug carrier systems, providing versatile clinical advantages and large scale production [5]. In addition to this, polymeric and lipid based hybrid nanoparticles (LPHNPs) have attained considerable attention to integrate the positive attributes and to overcome the possible drawbacks associated with drug delivery technologies. LPHNPs integrate the structural advantage of polymer and biomimetic properties of lipids, therefore enabling the improved dissolution profile of drugs [6]. LPHNPs can incorporate both hydrophilic and lipophilic drugs simultaneously [7]. The monolithic matrix system consists of drug particles dispersed homogeneously throughout lipid-polymer matrix [8]. . This unique structural design provides the mechanical integrity through maintaining the particle size, efficient drug loading and good biocompatibility [9]. Neverthless, polymeric nanoparticles and liposomes have been effectively used for drug delivery, but these carriers pose some drawbacks including stability and aggregation. . To address these problems associated with polymeric and liposomal drug delivery system, we report development of an alternative LPHNPs nanocarrier for dissolution enhancement of poorly water-soluble drug ICZ. Chitosan is a key polymer for drug delivery applications due to its biodegradability and economical nature [10]. Chitosan is a biocompatible polymer obtained from chitin [11]. Structurally, chitosan is a linear polysaccharide consisting of randomly distributed -(1 → 4)-linked D-glucosamine (deacetylated unit) and *N*-acetyl-D-glucosamine (acetylated unit) as shown in Fig. 1.

Glyceryl monostearate (GMS) was used as lipid for fabrication of LPHNPs. It has a single fatty acid chain attached to a glycerol backbone. Due to the amphiphilic nature, GMS molecules self-assemble both in water and oil into several types of mesophases [13]. GMS is a lipophilic surfactant generally recognized as safe (GRAS), with a broad range of applications from stabilizer to release agent [14]. Hydrophobic modification of the carrier might be an effective way to further improve the delivery of ICZ. We employed GMS, as the hydrophobic part since its fatty acid chains can interact with the phospholipids (structural part of the biological membrane) thereby leading to increased permeability [15]. The future studies can also be designed to explore the in-vivo enhanced permeation of ICZ with prepared LPHNPs.

Taking altogether these perspectives, the present study was aimed to develop LPHNPs for improving dissolution profile of ICZ. . Chitosan and GMS were employed in the study for fabrication of ICZ loaded LHNPs. Further, newly developed LPHNPs containing ICZ were characterized for compatibility, entrapment efficiency, particle size, polydispersity index (PDI), morphology, thermal behavior and dissolution profiles at biorelevant pH conditions.

2. Materials and methods

2.1. Materials

Itraconazole (ICZ) was gifted by Vision Pharmaceuticals (Pvt) Limited, Islamabad (Pakistan) as research material donation. Glyceryl monostearate (GMS), poloxamer 188, chitosan (CS), disodium hydrogen phosphate, sodium dihydrogen phosphate were purchased from Sigma-Aldrich (Germany). Methanol was acetic acid were purchased from Merck (Germany) Dialysis membranes (MWCO 12,000 to 14,000 Da) was procured from Sigma-Aldrich (Germany). The double distilled water was obtained from distillation plant installed at Riphah Institute of Pharmaceutical Sciences, Riphah International University, Lahore, Pakistan.

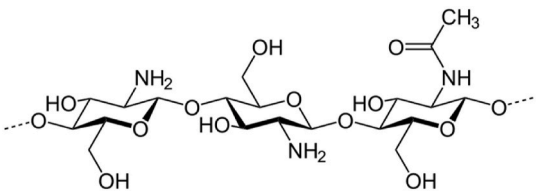

Fig. 1. Structure of Chitosan [12].

2.2. Preparation of LPHNPs loaded with ICZ

Itraconazole (ICZ) loaded lipid-polymer hybrid nanoparticles (LPHNPs) were prepared using solvent emulsification/diffusion technique with slight modification [16]. Accurately weighed amount (50 mg) of glyceryl monostearate (GMS) was dissolved in 5 mL methanol. ICZ (100 mg) was incorporated to this lipid solution (lipid phase) and heated to 70 °C in a water bath. The respective amount of chitosan (0.5 mg/mL) for each LPHNPs (Table 1) was dissolved in 0.1% acetic acid and filtered through 0.45 μm filter (Sartorius, Germany). Then chitosan solution was added to lipid phase and was heated to 70 °C again in water bath. For each LPHNPs formulation, the weighed amount of poloxamer 188 (Table 1) was mixed in 20 mL double distilled water (water phase). Then both lipid and aqueous phase were mixed and sonicated for 20 min at 70 °C. The LPHNPs were obtained by cooling nanoparticles in an ice water bath (2–3 °C) to quickly crystallize the lipid. The resultant ICZ loaded LPHNPs formulations were coded as LPHNPs-1, LPHNPs-2, LPHNPs-3, LPHNPs-4, LPHNPs-5, LPHNPs-6, LPHNPs-7 and LPHNPs-8 and stored at 4 °C for further characterization. The composition of LPHNPs is given in Table 1.

2.3. Optimization of LPHNPs

By using different ratios of the chitosan and poloxamer 188 with constant GMS concentration, ICZ-loaded LPHNPs were formulated (Table 1). The optimized GMS to chitosan and GMS to poloxamer 188 ratios were chosen on the basis of higher entrapment efficiency and small particle size.

2.4. Physicochemical characterization of LPHNPs

2.4.1. Drug-polymer interaction studies

The possible interactions between ICZ and LPHNPs formulation components were studied by attenuated total reflectance Fourier transform infrared (ATR-FTIR) spectroscopy (Shimadzu, Japan). ICZ, chitosan, GMS, poloxamer 188, LPHNPs-1 and LPHNPs-5 were subjected to FTIR measurements. Attenuated total reflectance (ATR) mode of spectrophotometer was operated and analytes were placed directly on diamond crystal. Spectral area analyzed was 400–4000 cm^{-1}. Ten scans were recorded for each measurement.

2.4.2. Entrapment efficiency (EE) studies

The percent entrapment efficiency (%EE) of ICZ loaded LPHNPs was determined using ultracentrifugation method reported elsewhere [17]. LPHNPs formulations were subjected to centrifugation at 15,000 rpm for 30 min at 4 °C using cooling centrifuge (DLab Scientific INC. USA). ICZ concentration in supernatant of LPHNPs was estimated using UV spectrophotometer (UV 1800 Shimdzu, Japan) at 262 nm %EE was calculated using following equation:

$$\%EE = \frac{Total\ amount\ of\ ICZ - Amount\ of\ free\ ICZ}{Total\ amount\ of\ ICZ} \times 100 \quad (1)$$

2.4.3. Particle size, polydispersity index and zeta potential

The average particle size, polydispersity index (PDI) and zeta potential of LPHNPs were determined at 25 °C using dynamic light scattering technique (Malvern, Zetasizer nano version 7.11, UK). The nanoparticle formulations (1 mL) were diluted with 10 mL distilled water prior to measurement. All measurements were performed in triplicate.

2.4.4. Scanning electron microscopy (SEM)

The morphology of optimized LPHNPs-1 and LPHNPs-5 (based on %EE and particle size) was examined using a field emission scanning electron microscope (FEI Nova Nano SEM 450, USA). 10 μL of optimized LPHNPs (LPHNPs-1 and LPHNPs-5) was mounted on an aluminum stub with adhesive silver tape. The stubs were stored overnight under the vacuum and then sputter-coated using gold. SEM was operated at an accelerated voltage of 10 kV with the magnification of 5000× and 1000×.

2.4.5. Differential scanning calorimetry

The physical state of ICZ in LPHNPs was investigated using differential scanning calorimetry (DSC). ICZ, chitosan, GMS, poloxamer

Table 1
Composition of ICZ loaded matrix LPHNPs.

Formulation Codes	Glyceryl monostearate (mg)	Chitosan (mg)	Poloxamer 188 (mg)
LPHNPs-1	50	25	30
LPHNPs-2	50	50	30
LPHNPs-3	50	75	30
LPHNPs-4	50	100	30
LPHNPs-5	50	25	25
LPHNPs-6	50	25	20
LPHNPs-7	50	25	15
LPHNPs-8	50	25	10

188, LPHNPs-1 and LPHNPs-5 were subjected to DSC measurement using DSC Q200 (TA Instruments, DE, USA).

The DSC instrument was calibrated with Indium (melting point = 157.6 °C) for the temperature and heat flow. All the test samples were weighed accurately (2–6 mg) and hermetically sealed in the aluminum pans. The loaded aluminum pans were compared with the empty aluminum pan as a reference. The samples were heated at a heating rate of 10 °C/min from 25 to 250 °C under the inert atmosphere of nitrogen at a purging rate of 50 mL min^{-1}.

2.4.6. Dissolution studies of LPHNPs

ICZ dissolution from LPHNPs was carried out in biorelevant acidic medium; 0.1 N HCl (pH 1.2) and biorelevant basic medium; phosphate buffer (pH 7.4) respectively using dialysis bag method [18]. Initially, bags were soaked in distilled water for 12 h prior to use. 2 mL of LPHNPs formulation was poured into the dialysis bag with the two ends tightened by thread knots. The dialysis bag was placed in a beaker containing 100 mL of dissolution medium. The beaker was placed over a magnetic stirrer at 37 °C at a speed of 100 rpm. For studying dissolution at acidic pH, aliquots of 2 mL were taken at predefined time intervals i.e. 0.25, 0.5, 1, 1.5 and 2 h and replenished with equal amount of fresh dissolution medium. The samples were assayed for ICZ content at λ_{max} of 258 nm. Similarly, at basic pH conditions, aliquots of 2 mL were withdrawn at predefined time intervals 0.5, 1, 2, 4, 6, 8, 10 and 12 h and replenished with equal amount of fresh dissolution medium. The samples were analyzed using UV spectrophotometer (UV 1800 Shimadzu, Japan) at 262 nm [19].

2.4.7. Kinetic modelling of dissolution data

To assess the correlation coefficient (r^2) and dissolution kinetics of ICZ loaded LPHNPs, the *in-vitro* drug dissolution data was subjected to different kinetic models. This was achieved by plotting the drug concentration (Q) against time (t). Following models including zero order (Eq. (i)), first order (Eq. (ii)), Higuchi model (Eq. (iii)) and Korsemyer-peppas model (Eq. (iv)) were applied to find out mechanism of drug dissolution.

Zero order

$$Q = Q_o + kt \quad \text{(i)}$$

First order

$$Q = Q_0 + ket \quad \text{(ii)}$$

Higuchi equation

$$Q = k \times t_{0.5} \quad \text{(iii)}$$

Korsmeyer–Peppas equation

$$Q = K \times t_n \quad \text{(iv)}$$

where Q denotes the quantity dissolved of the drug in time t, Q_0 denotes the value of Q at time zero, k represents the release rate constant and "n" signifies the release exponent. The model that displayed a linear plot and showed the highest value of (r^2) was considered as the best-fit model [20].

2.5. Statistical analysis

The experiments were performed in triplicate. The results were illustrated as mean ± SD. The data obtained from repeated measurements were subjected to one-way ANOVA and a value of $p < 0.05$ was considered as significant.

3. Results and discussion

3.1. Preparation of LPHNPs

LPHNPs loaded with ICZ were prepared successfully using solvent emulsification/diffusion method. Chitosan, GMS and poloxamer 188 were utilized as polymer, lipid and stabilizer respectively for preparation of nanoparticles.

The emulsification/diffusion method involves rapid diffusion of the solvent into non-solvent phase which decreases the interfacial tension between the two phases and increase the surface area which leads to the formation of nanoparticles [21]. Due to the spontaneous diffusion of the solvent, interfacial turbulence occurs between the aqueous and lipid phases, leading to the formation of nanoparticles. The technique has been reported to be efficient, versatile, easy to implement and allows a high entrapment efficiency of lipophilic drugs in polymeric matrices [22]. Emulsification-solvent diffusion method is able to produce hybrid nanoparticles with high encapsulation efficiency, good yields, no need of high shear ultrasonication and batch-to-batch reproducibility [23]. In the current study, ICZ loaded LPHNPs were developed using solvent diffusion technique to improve solubility and dissolution profile of the drug. The eight formulations were divided into two groups on the basis of varying concentration of chitosan and poloxamer 188. In group-I (LPHNPs-1, LPHNPs-2, LPHNPs-3 and LPHNPs-4), the effects of chitosan were studied with varying concentration from 25 mg to 100 mg, whereas in group-II (LPHNPs-5, LPHNPs-6, LPHNPs-7 and LPHNPs-8), the effects of poloxamer 188 were studied with decreasing concentration from 25 mg to 10 mg. Considering the above advantages, in the present work, the feasibility of using the

emulsification/diffusion method to prepare ICZ loaded LPHNPs was evaluated. . The other key parameters such as lipophilicity (the influence of lipid self-emulsification properties, lipid shape and surface area) and lipid crystallization rate of nanoparticle preparation will be different for different lipids [24]. GMS was used as a solid lipid in this study, to form the fatty core in the LPHNPs. GMS (melting point ~60 °C), when heated to 10 °C above the melting point, will react hydrophobically with drug molecules thus trapping the drug molecules on cooling. GMS is a safe lipid with sufficient biocompatibility and less toxic for the human body [23]. Due to the modification within the lipids, GMS provides an efficient incorporation of the drugs, thus achieving the sustainable properties of the LPHNPs. Poloxamer 188 stabilizes the nanoparticle by forming a coating around the lipid core of the incorporated drug [25]. LPHNPs-1 and LPNPs-5 were considered optimized formulations on the basis of greater entrapment efficiency and small particle size.

3.2. Drug polymer interaction studies

FTIR spectra of pure drug ICZ, chitosan GMS, poloxamer 188, LPHNPs-1 and LPHNPs-5 are shown in Fig. 2. FTIR spectrum of ICZ showed the characteristic peaks at 3127.1 cm^{-1}, 3068.5, 2936.0 cm^{-1}, 2823.6 cm^{-1}, 1698.4 cm^{-1}, 1510.8 cm^{-1} and 1451.3 cm^{-1}. The transmittance bands between 2800 and 3200 cm^{-1} were 325 corresponded to the alkane, aromatic CH and amine groups [26]. The transmittance peaks of the NH2 groups were located at 3442.0 cm^{-1}, 3127.1 cm^{-1} and 3068.5 cm^{-1}. The first band was assigned to be due to stretching vibration of free *N*–H in drug molecule. The other two transmittance bands were 328 cm^{-1} caused by the amino group and the sharp peak occurring at 1698.4 cm^{-1} was due to C═O of the drug. This is in agreement with the previously reported spectrum of the pure drug [27]. The IR spectrum of poloxamer 188 is characterized by principal transmittance peaks at 2883 cm^{-1} (C–H stretch aliphatic), 1341 cm^{-1} (in-plane O–H bend) and 1099 cm^{-1} (C–O stretch). Similarly, spectrum of pure GMS showed transmittance peaks of OH stretching at 3300 cm^{-1}, C–H stretching at 2914.38 cm^{-1}, C═O stretching at 1729.82 cm^{-1} and C–H bending at 1469.06 cm^{-1}. This could be due to long $–CH_2$ chain length and -CH2 bending at 1178 cm^{-1} and 718 cm^{-1}. A transmittance band at 3419 cm^{-1} corresponds to the combined peaks of the NH_2 and OH group stretching vibration in chitosan. The transmittance band at 1657 cm^{-1} is attributed to the -CONH2 group [28]. FTIR spectra of LPHNPs-1 and LPHNPs-5 were observed to be different. FTIR spectra of LPHNPs (Fig. 2) showed the remarkable attenuation of IR bands of drug and polymers with significant reduction in the intensity of peaks. Most of the peaks were found to be diffused indicating formation of LPHNPs. Moreover, major peaks of ICZ were smooth indicating strong physical interaction between drug and polymers. No additional peaks or shifting of peaks was observed nanoparticle formulations indicating no chemical interaction between drug, polymers and lipids.

FTIR analysis is performed to reveal chemical interactions within the constituent formulations. The FTIR spectrum of ICZ demonstrated the characteristic peaks at 2821.95 cm^{-1}, 3130.57 cm^{-1} due to C–H- stretching vibrations. The disappearance of the characteristic peak of ICZ in the formulations LPHNPs-1 and LPHNPs-5 indicates that ICZ has been successfully incorporated into the LPHNPs. Similarly, the characteristic peaks of GMS, chitosan and poloxamer 188 are also slightly shifted from their original values which further indicated drug incorporation. The results showed that there is no significant chemical interaction between LPHNPs components and the drug.

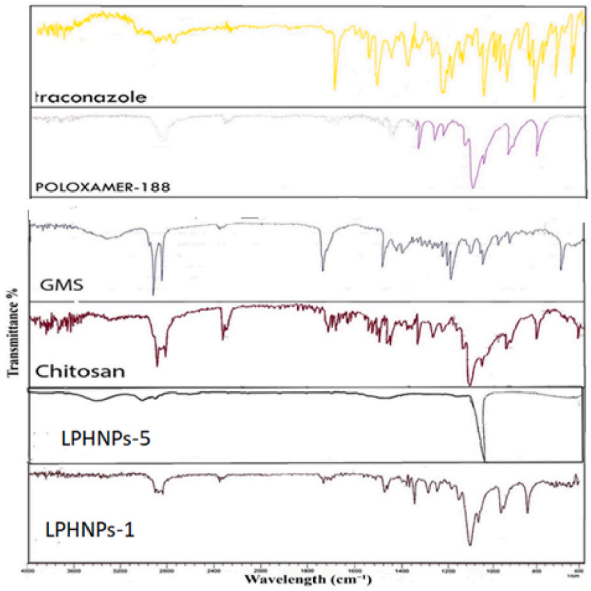

Fig. 2. FTIR spectra of LPHNPs-1, LPHNPs-5, Chitosan, GMS, Poloxamer-188 and ICZ.

3.3. Entrapment efficiency % (%EE)

The percent entrapment efficiency (%EE) of ICZ loaded LPHNPs was found to be in range of 85.21%–91.34% for nanoparticles coded as LPHNPs-1 to LPHNPs-4 which contained varying concentrations of chitosan whereas nanoparticles coded as LPHNPs-5 to LPHNPs-8 showed % EE values in range 78.32%–90.44%. The optimized formulations LPHNPs-1 and LPHNPs-5 demonstrated maximum %EE of ICZ. These results showed superiority of developed LPHNPs as %EE of formulation acts as a determining factor for dose volume to be administered for desired therapeutic effect. The high %EE achieved might be due to conjugation of GM with backbone of chitosan. The %EE of all LPHNPs formulations is shown in Table 2.

Higher values of %EE for ICZ were attained in this study indicating superiority of LPHNPs for delivery of ICZ This may be due to the presence of long chain fatty acids in structure of GMS which resulted in increased %EE of lipophilic drug i. e ICZ [26]. In this method of preparation, drug is well dissolved in molten lipid at temperature above the melting point of lipid and there is less drug leakage or precipitation of drug during the preparation. The emulsification step using poloxamer 188 as stabilizer has provided sufficient integrity to the LPHNPs. The %EE of LPHNPs was decreased non-significantly with increase in chitosan concentration ($p > 0.05$). It is reported that chitosan has strong affinity for the phospholipid group of the prepared formulations [11]. On the contrary, direct relationship was observed between poloxamer 188 concentration and %EE. The decrease in poloxamer 188 concentration decreased the %EE, non-significant differences were observed among the LPHNPs-4 to LPHNPs-8 ($p > 0.05$). The role of poloxamer 188 is to stabilize the hybrid nanoparticle system. The addition of this thermodynamically stabilized emulsion to high viscosity chitosan solution resulted in higher EE [29]. This may be due to increase in solubility of ICZ in the lipid on increasing the concentration of poloxamer 188. These finding were in agreement with previous findings reported by Abdelbari et al. [30].

3.4. Particle size, polydispersity index and zeta potential

Particle size of developed matrix LPHNPs with varying concentration of chitosan (LPHNPs-1 LPHNPs-2, LPHNPs-3 and LPHNPs-4) was found to be in range of 421–588 nm whereas size was observed in 489–725 nm range for LPHNPs-5, LPHNPs-6, LPHNPs-7 and LPHNPs-8 respectively. With increasing concentration of chitosan at constant poloxamer 188 (stabilizer) concentration in first five LPHNPs formulations (LPHNPs-1 – LPHNPs-5), the particle size was also increased. There are multiple factors which can affect particle size of nanoparticles. This includes concentration and molecular weight of chitosan. A linear relationship was seen where increase in chitosan concentration caused increase the size of particles. This increase in the particle size at higher concentrations of chitosan might be due to the increase in the viscosity of the resultant dispersion that have been attributed in two different ways. Firstly, the increase in the viscosity decrease the evaporation rate of the organic solvent, resulting into the larger particle size [31]. Secondly, the viscosity at higher polymer concentration also poses a hindrance to the size reduction of droplets into smaller particles and decreases the effect of shear force produced by the sonication/stirring [32]. Similar results were attained in previous studies, which further supported by the Stock's law. According to that, differences in the viscosity of dispersion medium resist the particles collision and might decrease the chances of breakdown into smaller particles [33]. The effect of poloxamer 188 was inverse to that of chitosan. Keeping chitosan concentration constant and decreasing concentration of poloxamer in LPHNPs-5 to LPHNPs-8, caused increase in particle size. Poloxamer 188, being a surfactant, stabilizes the emulsion, formed after diffusion of the organic solvent in the aqueous phase, by decreasing the interfacial tension between the two phases. Higher concentration of poloxamer 188 effectively stabilizes the emulsion, ultimately reducing particle size of LPHNPs [29]. The optimized formulations showed average particle size 421 nm and 489 nm respectively with PDI value 0.34. Particle size is critical determinant for the fate of orally administered nanoparticles. The smaller particle size can improve bioadhesion of nanoparticles, prolong residence time and thus play a contributing role in improving oral bioavailability [34]. In addition, the cellular uptake and uptake pathway of particles are also affected by the size of nanoparticles. Our studies were limited to evaluate in-vitro characteristics of ICZ loaded LPHNPs. Therefore, this study can be further extended in future to evaluate bioavailability of ICZ using animal models or cell uptake studies of LPHNPs-1 and LPHNPs-2 studies intestinal Caco-2 cells. The term "polydispersity" (or "dispersity" as recommended by IUPAC) is used to describe the degree of non-uniformity of a size distribution of particles [35]. . PDI values were found to be 0.34–0.56 for LPHNPs-1 to LPHNPs-4 and 0.34–0.74 for LPHNPs-5 to LPHNPs-8. The results showed that increased chitosan concentration can induce an agglomeration of nanoparticles resulting in higher PDI values. Poloxamer 188, as a non-ionic emulsifier, may somewhat act as a co-emulsifier in the fabrication process, resulted in smaller particle size and narrower size distribution. When used as a stabilizer, poloxamer 188 provides additional steric stabilization effect preventing aggregation of the fine particles in the colloidal system [36]. The zeta potential also increases the stability of the

Table 2
Entrapment efficiency values of LPHNPs.

Formulation codes	% Entrapment efficiency
LPHNPs-1	91.34 ± 1.1
LPHNPs-2	89.75 ± 1.1
LPHNPs-3	88.13 ± 1.5
LPHNPs-4	85.21 ± 2.4
LPHNPs-5	90.44 ± 1.5
LPHNPs-6	86.56 ± 1.7
LPHNPs-7	82.44 ± 2.9
LPHNPs-8	78.32 ± 2.6

preparation by imparting a charge on the surface of the nanocarrier, thus avoiding aggregation within the preparation. Zeta potential determination is a significant characterization technique of nanoparticles to estimate the surface charge, which can be employed for understanding the physical stability [37]. The zeta potential usually in the range 10 mV–25 mV, can provide sufficient stability to the nanoformulation. t (Yuan et al., 2008). The zeta potential values was in range of 7.75–22.8 mV for LPHNPs-1 to LPHNPs-4 and 10.5–21.60 mV for LPHNPs-5 to LPHNPs-8 hybrid nanoparticles. Positive zeta potentials were obtained for all samples in the presence of chitosan polymer with free positively-charged groups. These results are presented in Table 3.

3.5. Scanning electron microscopy (SEM)

SEM images of optimized LPHNPs (LPHNPs-1 and LPHNPs-5) revealed oval shape of particles as shown in Fig. 3A and B. The sizes of particles measured by SEM, as can be observed from Fig. 3A and B, were larger than that recorded by zetasizer. This variation in particle size measurement can be ascribed to slight aggregation in nanoparticle samples during preparation.

3.6. Differential scanning calorimetry (DSC)

The DSC thermograms of LPHNPs-1, ICZ, GMS, chitosan and poloxamer 188 are shown in Fig. 4. .

The thermal behavior of LPHNPs was evaluated using DSC technique which showed the melting characteristics of the LPHNPs and its formulation components. It is a tool that gives an insight into the melting and recrystallization behavior of crystalline materials like LPHNPs [30]. DSC thermogram of crystalline ICZ showed a single sharp melting endothermic peak at 180 °C (Fig. 4A) close to its intrinsic melting point (168 °C). The chitosan polymer typically demonstrated an endothermic peak at 125 °C. This observation is in agreement with another study reported previously [38]. Chitosan usually has strong affinity for water molecules and in solid state these molecules may have disordered structures. This endothermic peak of chitosan (Fig. 4D) corresponds to the evaporation of bound water from the pure chitosan. The thermal curves of GMS demonstrated an endothermic invagination at around 68 °C, ICZ at 65 °C, poloxamer 188 at around 54 °C. DSC thermograms of ICZ-loaded LPHNPs-1 showed absence of characteristic peak of ICZ compared to the pure drug, which suggested that ICZ could be present in an amorphous form in the LPHNPs, this behavior is expected to improve the solubility of the drug in water resulting in improved dissolution profile. Further, the absence of sharp peak has been suggested to be due to the strong interaction with the lipid component of the LPHNPs.

3.7. Dissolution studies of LPHNPs

Dissolution of ICZ from LPHNPs-1 and LPHNPs-5 was compared with the dissolution of control (aqueous dispersion of pure ICZ) in biorelevant acid medium (0.1 N HCl, pH 1.2) and biorelevant basic medium (phosphate buffer, pH 7.4). The in vitro dissolution profiles are depicted in Fig. 5. The percent drug dissolved was higher for tested LPHNPs compared to the control in both the dissolution media (Fig. 5A and B). At pH 1.2, the drug dissolved after 2 h by LPHNPs-1, LPHNPs-5 and ICZ aqueous dispersion was 23.3%, 19.18% and 11.32% respectively. The prepared LPHNPs revealed improvement in dissolution profile compared to aqueous dispersion of pure drug at acidic pH. At acidic conditions, burst dissolution of the drug was not observed (Fig. 5A). These results indicated the advantages of prepared LPHNPs at acidic pH as burst dissolution can cause drug concentrations near or above the toxic level in vivo leading to dose dumping. Furthermore, drug dissolved during burst stage may also be metabolized and excreted without being effectively utilized [39]. These findings indicated stronger intermolecular interactions between matrix components including ICZ, chitosan, glyceryl monostearte and poloxamer 188. The pH dependent dissolution profile of LPHNPs-1 and LPHNPs-5 shows a slow drug dissolution at acidic pH that ascended to a quick dissolution upon changing the pH. Furthermore, the stabilizing effect of the poloxamer 188 in LPHNps prevents the escape of the drug from the matrix in an irregular manner. The mixture of surfactant and poloxamer 188 provides sufficient rigidity to the structure and immobilizes the drug in the matrix system. The other factors which may likely to contribute to slow dissolution of drug at acidic pH are high viscosity in matrix and long diffusion distances for the drug [40]. In addition to this, lower amounts of ICZ dissolved from LPHNPs at acidic could be due to physical entanglement of drug inside multicomponent matrix LPHNPs. The slower drug dissolution rate in the acidic pH than the alkaline pH is attributed to the repulsion between H+ ions and cations of chitosan, which slow down the hydrolysis [41].

At pH 7.4, the drug dissolved after 12 h by LPHNPs-1, LPHNPs-5 and ICZ aqueous dispersion was 90.2%, 83.4% and 40.0%

Table 3
Particle size, polydispersity index and zeta potential values of LPHNPs.

Formulation codes	Particle size (nm)	Polydispersity index (PDI)	Zeta potential (mV)
LPHNPs-1	421 ± 6.1	0.34 ± 0.1	22.8 ± 2.45
LPHNPs-2	465 ± 7.7	0.46 ± 0.2	10.9 ± 1.86
LPHNPs-3	561 ± 8.24	0.56 ± 0.1	13.9 ± 1.92
LPHNPs-4	588 ± 9.80	0.59 ± 0.2	7.75 ± 0.99
LPHNPs-5	489 ± 4.8	0.34 ± 0.4	21.6 ± 2.12
LPHNPs-6	617 ± 5.25	0.45 ± 0.3	13.0 ± 1.64
LPHNPs-7	716 ± 6.16	0.51 ± 0.2	11.2 ± 1.32
LPHNPs-8	725 ± 3.69	0.74 ± 0.1	10.5 ± 1.47

Results are presented as ± SD.

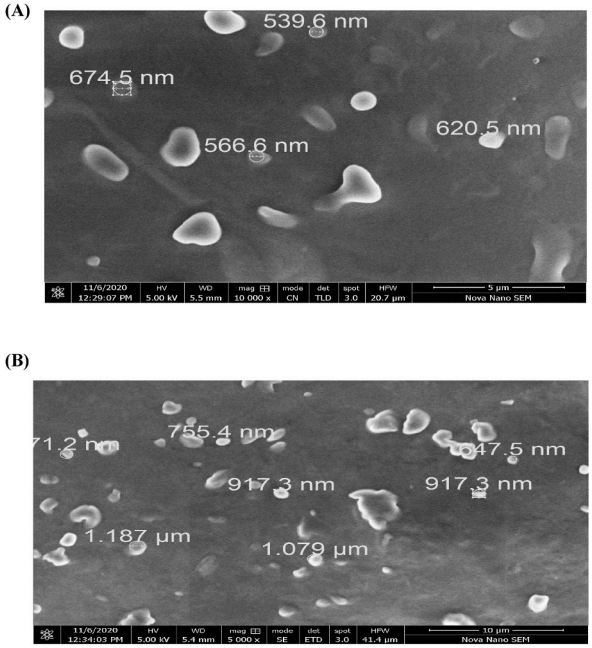

Fig. 3. SEM images of ICZ loaded matrix LPHNPs (A) LPHNPs-1 (B) LPHNPs-5.

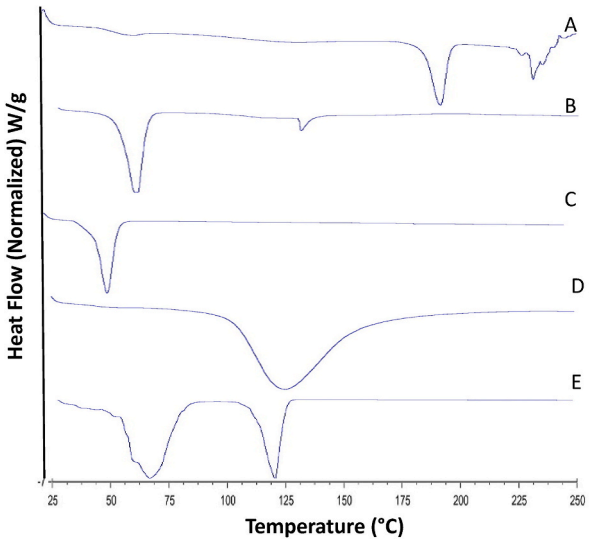

Fig. 4. DSC thermograms of Itraconazole (A), Glyceryl monostearate (B), Poloxamer 188 (C), chitosan (D) and matrix LPHNPs-1 (E).

respectively (Fig. 5B). There were significant differences of drug dissolution rates of LPHNPs-1 and LPHNPs-5 compared to ICZ aqueous dispersion at 12 h as demonstrated in Fig. 5B ($p < 0.05$). The high drug availability in the basic medium corresponds to the effect of formulation components in enhancing the solubility of ICZ. The faster drug dissolution from LPHNPs-1 compared to LPHNPs could be attributed to high concentration of poloxamer 188 in former [42]. Furthermore, higher amounts of ICZ dissolved can be explained by the decrease in the interfacial tension and the expected increase in ICZ wettability due to poloxamer 188 [43]. Poloxamer 188 remarkably increased dissolution profile of ICZ at basic pH owing to its surface active properties [44]. To develop ICZ loaded LPHNPs as a platform technology for fungal infections, our future studies are aimed at evaluating the in-vivo pharmacokinetics and in-vivo efficacies of the LPHNPs in animal models.

3.8. Kinetic modelling of dissolution data

Various kinetic models were applied to the *in-vitro* dissolution patterns of ICZ from LPHNPs-1 and LPHNPs-5. R^2 values for each

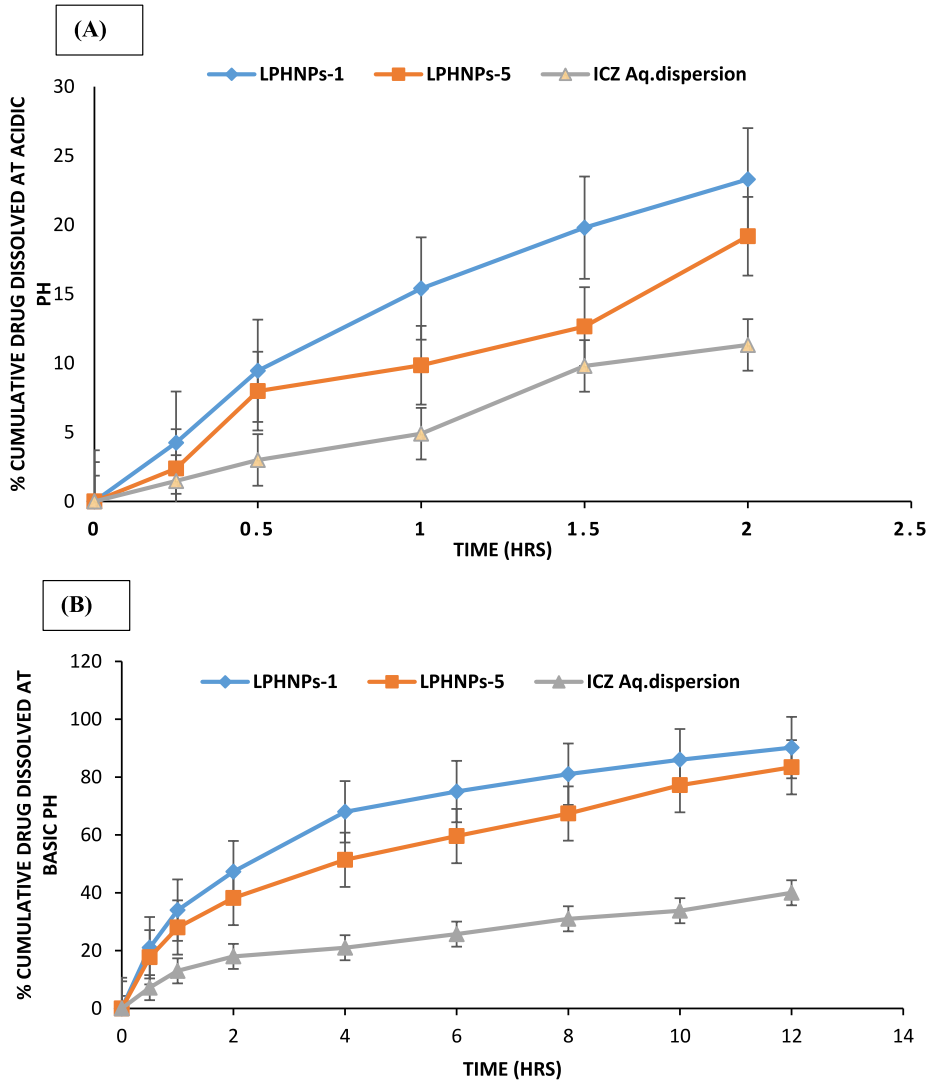

Fig. 5. Dissolution Profiles of ICZ from LPHNPs at acidic pH (A) and basic pH.

applied model are presented in Tables 4 and 5. Korsmeyer-Peppas model was found to be the best fit owing to its highest R^2 values for in-vitro drug dissolution of LPHNPs-1 and LPHNPs-5. At acidic pH conditions, the "n" value for ICZ in LPHNPs-1 and LPHNPs-5 were found to be 0.70 and 0.80, respectively, displaying dissolution via non-fickian diffusion model. At basic pH conditions, the "n" value for ICZ in LPHNPs-1 and LPHNPs-5 were found to be 0.39 and 0.45, respectively, displaying dissolution via fickian diffusion model.

4. Conclusion

Matrix type LPHNPs loaded with ICZ were developed successfully to improve ICZ dissolution profile. Solvent emulsification/diffusion technique was utilized successfully for the preparation of ICZ loaded matrix LPHNPs. Chitosan and poloxamer 188 with varying content level significantly affected the various physicochemical characteristic of LPHNPs. The optimized LPHNPs-1 (minimum chitosan concentration) and LPHNPs-5 (maximum poloxamer concentration) yielded nanoparticles with improved physicochemical characteristics such as small particle size, higher entrapment efficiency and improved dissolution profile. The dissolution of ICZ from matrix LPHNPs followed Korsmeyer-peppas model. The overall results of the study suggested that suitable combinations of chitosan and poloxamer 188 with GMS have potential to act as alternate carriers for oral delivery of ICZ.

Funding

This research was not funded by any funding agency.

Table 4
Dissolution kinetics of ICZ from LPHNPs-1 and LPHNPs-5 at acidic conditions.

LPHNPS	Zero order		First order		Higuchi model		Korsmeyer-peppas		
	K	R^2	K	R^2	K	R^2	K	R^2	n
LPHNPs-1	12.89	0.94	0.146	0.96	15.50	0.95	14.66	0.99	0.70
LPHNPs-5	9.49	0.94	0.10	0.95	11.29	0.89	10.31	0.98	0.80

Table 5
Dissolution kinetics of ICZ from LPHNPs-1 and LPHNPs-5 at basic pH conditions.

LPHNPs	Zero order		First order		Higuchi model		Korsmeyer-peppas		
	K	R^2	K	R^2	K	R^2	K	R^2	n
LPHNPs-1	9.45	0.56	0.27	0.95	28.71	0.96	35.57	0.98	0.39
LPHNPs-5	8.12	0.72	0.16	0.93	24.52	0.97	26.97	0.99	0.45

Reviewer disclosures

Peer reviewers on this manuscript have no relevant financial or other relationships to disclose.

Declaration of competing interest

M.F. Akhtar is the member of advisory board of Heliyon journal. The authors have no relevant affiliations or financial involvement with any organization or entity with a financial interest in or financial conflict with the subject matter or materials discussed in the manuscript. This includes employment, consultancies, honoraria, stock ownership or options, expert testimony, grants or patents received or pending, or royalties.

Acknowledgments

As a thesis research project, this study was supported by Riphah International University, Lahore campus.

References

[1] L. Willems, R. Van der Geest, K. De Beule, Itraconazole oral solution and intravenous formulations: a review of pharmacokinetics and pharmacodynamics, J. Clin. Pharm. Therapeut. 26 (3) (2001) 159–169.
[2] J. Peeters, et al., Characterization of the interaction of 2-hydroxypropyl-β-cyclodextrin with itraconazole at pH 2, 4, and 7, J. Pharmaceut. Sci. 91 (6) (2002) 1414–1422.
[3] K. Chowdary, S.S. Rao, Investigation of dissolution enhancement of itraconazole by solid dispersion in superdisintegrants, Drug Dev. Ind. Pharm. 26 (11) (2000) 1207–1211.
[4] C. Timpe, Drug solubilization strategies applying nanoparticulate formulation and solid dispersion approaches in drug development, Pharm. Rev. 13 (2010) 12–21.
[5] T.M. Allen, P.R. Cullis, Liposomal drug delivery systems: from concept to clinical applications, Adv. Drug Deliv. Rev. 65 (1) (2013) 36–48.
[6] M.M. Khan, et al., Co-delivery of curcumin and cisplatin to enhance cytotoxicity of cisplatin using lipid-chitosan hybrid nanoparticles, Int. J. Nanomed. 15 (2020) 2207.
[7] L. Zhang, et al., Self-assembled lipid− polymer hybrid nanoparticles: a robust drug delivery platform, ACS Nano 2 (8) (2008) 1696–1702.
[8] X.Y. Wu, Strategies for optimizing polymer-lipid hybrid nanoparticle-mediated drug delivery, Expet Opin. Drug Deliv. 13 (5) (2016) 609–612.
[9] B. Mandal, et al., Development and in vitro evaluation of core–shell type lipid–polymer hybrid nanoparticles for the delivery of erlotinib in non-small cell lung cancer, Eur. J. Pharmaceut. Sci. 81 (2016) 162–171.
[10] Q. Hu, et al., Biocompatible polymeric nanoparticles with exceptional gastrointestinal stability as oral delivery vehicles for lipophilic bioactives, Food Hydrocolloids 89 (2019) 386–395.
[11] J.-x. Guo, et al., Chitosan-coated liposomes: characterization and interaction with leuprolide, Int. J. Pharm. 260 (2) (2003) 167–173.
[12] V. Mikušová, P. Mikuš, Advances in chitosan-based nanoparticles for drug delivery, Int. J. Mol. Sci. 22 (17) (2021) 9652.
[13] P. Talele, S. Sahu, A.K. Mishra, Physicochemical characterization of solid lipid nanoparticles comprised of glycerol monostearate and bile salts, Colloids Surf. B Biointerfaces 172 (2018) 517–525.
[14] A.S. de Sousa, et al., Preparation of glyceryl monostearate-based particles by PGSS®—application to caffeine, J. Supercrit. Fluids 43 (1) (2007) 120–125.
[15] T. Sonia, M. Rekha, C.P. Sharma, Bioadhesive hydrophobic chitosan microparticles for oral delivery of insulin: in vitro characterization and in vivo uptake studies, J. Appl. Polym. Sci. 119 (5) (2011) 2902–2910.
[16] Y. Luo, et al., Solid lipid nanoparticles for oral drug delivery: Chitosan coating improves stability, controlled delivery, mucoadhesion and cellular uptake, Carbohydr. Polym. 122 (2015) 221–229.
[17] M.I. Khan, A. Madni, L. Peltonen, Development and in-vitro characterization of sorbitan monolaurate and poloxamer 184 based niosomes for oral delivery of diacerein, Eur. J. Pharmaceut. Sci. 95 (2016) 88–95.
[18] M.I. Khan, et al., Ultrasonic processing technique as a green preparation approach for diacerein-loaded niosomes, AAPS PharmSciTech 18 (5) (2017) 1554–1563.
[19] A. Karagianni, L. Peltonen, Production of itraconazole nanocrystal-based polymeric film formulations for immediate drug release, Pharmaceutics 12 (10) (2020) 960.
[20] M.I. Khan, et al., Formulation design and characterization of a non-ionic surfactant based vesicular system for the sustained delivery of a new chondroprotective agent, Braz. J. Pharm. Sci. 51 (3) (2015) 607–615.
[21] J.P. Rao, K.E. Geckeler, Polymer nanoparticles: preparation techniques and size-control parameters, Prog. Polym. Sci. 36 (7) (2011) 887–913.

[22] D. Quintanar-Guerrero, et al., Adaptation and optimization of the emulsification-diffusion technique to prepare lipidic nanospheres, Eur. J. Pharmaceut. Sci. 26 (2) (2005) 211–218.
[23] H. Weyhers, et al., Solid lipid nanoparticles (SLN) - effects of lipid composition on in vitro degradation and in vivo toxicity, Pharmazie 61 (2006) 539–544.
[24] R.K. Subedi, K.W. Kang, H.-K. Choi, Preparation and characterization of solid lipid nanoparticles loaded with doxorubicin, Eur. J. Pharmaceut. Sci. 37 (3) (2009) 508–513.
[25] R.H. Müller, K. Mäder, S. Gohla, Solid lipid nanoparticles (SLN) for controlled drug delivery - a review of the state of the art, Eur. J. Pharm. Biopharm. 50 (1) (2000) 161–177.
[26] V.K. Venishetty, et al., Design and evaluation of polymer coated carvedilol loaded solid lipid nanoparticles to improve the oral bioavailability: a novel strategy to avoid intraduodenal administration, Colloids Surf. B Biointerfaces 95 (2012) 1–9.
[27] S.-Y. Shim, et al., Characterization of itraconazole semisolid dosage forms prepared by hot melt technique, Arch Pharm. Res. 29 (11) (2006) 1055–1060.
[28] L. Qi, et al., Preparation and antibacterial activity of chitosan nanoparticles, Carbohydr. Res. 339 (16) (2004) 2693–2700.
[29] P. Girotra, S.K. Singh, G. Kumar, Development of zolmitriptan loaded PLGA/poloxamer nanoparticles for migraine using quality by design approach, Int. J. Biol. Macromol. 85 (2016) 92–101.
[30] G. Abdelbary, R.H. Fahmy, Diazepam-loaded solid lipid nanoparticles: design and characterization, AAPS PharmSciTech 10 (1) (2009) 211–219.
[31] P.R. Ravi, et al., Design, optimization and evaluation of poly-ϵ-caprolactone (PCL) based polymeric nanoparticles for oral delivery of lopinavir, Drug Dev. Ind. Pharm. 41 (1) (2015) 131–140.
[32] B. Gajra, R.R. Patel, C. Dalwadi, Formulation, optimization and characterization of cationic polymeric nanoparticles of mast cell stabilizing agent using the Box–Behnken experimental design, Drug Dev. Ind. Pharm. 42 (5) (2016) 747–757.
[33] R.R. Patel, et al., Rationally developed core–shell polymeric-lipid hybrid nanoparticles as a delivery vehicle for cromolyn sodium: implications of lipid envelop on in vitro and in vivo behaviour of nanoparticles upon oral administration, RSC Adv. 5 (93) (2015) 76491–76506.
[34] Y. Wang, et al., The influence of nanoparticle properties on oral bioavailability of drugs, Int. J. Nanomed. 15 (2020) 6295.
[35] M. Danaei, et al., Impact of particle size and polydispersity index on the clinical applications of lipidic nanocarrier systems, Pharmaceutics 10 (2) (2018) 57.
[36] F. Yan, et al., The effect of poloxamer 188 on nanoparticle morphology, size, cancer cell uptake, and cytotoxicity, Nanomed. Nanotechnol. Biol. Med. 6 (1) (2010) 170–178.
[37] E. Joseph, G. Singhvi, Multifunctional Nanocrystals for Cancer Therapy: a Potential Nanocarrier. Nanomaterials for Drug Delivery and Therapy, 2019, pp. 91–116.
[38] A.R. Dudhani, S.L. Kosaraju, Bioadhesive chitosan nanoparticles: preparation and characterization, Carbohydr. Polym. 81 (2) (2010) 243–251.
[39] X. Huang, C.S. Brazel, On the importance and mechanisms of burst release in matrix-controlled drug delivery systems, J. Contr. Release 73 (2–3) (2001) 121–136.
[40] M. Kaur, et al., A green approach for the synthesis of silver nanoparticle-embedded Chitosan bionanocomposite as a potential device for the sustained release of the itraconazole drug and its antibacterial Characteristics, Polymers 14 (9) (2022) 1911.
[41] A. Dev, et al., Preparation of poly (lactic acid)/chitosan nanoparticles for anti-HIV drug delivery applications, Carbohydr. Polym. 80 (3) (2010) 833–838.
[42] T. Kazim, et al., Chitosan hydrogel for topical delivery of ebastine loaded solid lipid nanoparticles for alleviation of allergic contact dermatitis, RSC Adv. 11 (59) (2021) 37413–37425.
[43] N.S. Lotfy, T.M. Borg, E.A. Mohamed, The promising role of Chitosan–poloxamer 188 nanocrystals in improving diosmin dissolution and therapeutic efficacy against ferrous sulfate-induced hepatic injury in rats, Pharmaceutics 13 (12) (2021) 2087.
[44] A.V. Shah, A.T. Serajuddin, Development of solid self-emulsifying drug delivery system (SEDDS) I: use of poloxamer 188 as both solidifying and emulsifying agent for lipids, Pharmaceut. Res. 29 (2012) 2817–2832.